Research Article

Israel Journal of Chemistry

doi.org/10.1002/ijch.202100102

Design of MOFs with Absolute Structures: A Case Study

Haoze Wang+,[a, b] Xiaokun Pei+,[a, b] Davide M. Proserpio,[c, d] and Omar M. Yaghi*[a, b]

Dedicated to Professor Meir Lahav and Professor Leslie Leiserowitz for the Wolf Prize in Chemistry

Abstract: Metal-organic frameworks (MOFs) with absolute structures are of particular interest as the asymmetry of their crystal structures enables wide applications from asymmetric catalysis to enantioselective separation. Previous reports on the synthetic strategies toward MOFs with absolute structures always required the use of chiral precursors or chiral templates, however, it is not always easy to obtain enantiopure starting materials. Here in, we report a new non-centrosymmetric MOF, MOF-829, synthesized from aluminium salt and achiral organic linker. Further comparisons are made between MOF-829 and a reported Al-based chiral MOF (MOF-520) that is composed of the same metal ion and linker, and similarly synthesized without using chiral compounds. The configurations of the building units, the absolute structures of both MOFs, and their topologies were investigated in detail. We found that (i) topology is one of the determining factors in the formation of non-centrosymmetric MOFs; (ii) the formation of chiral MOFs further requires the directionality of chiral linkers but more importantly chiral secondary building units (SBUs), which can be realized by fine tuning of the synthetic conditions. We envision that both synthetic exploration of chiral SBUs and the design of non-centrosymmetric topologies will open a new direction in the design of MOFs with absolute structures.

Keywords: Metal–Organic Frameworks · Absolute Sturctures · Chirality

1. Introduction

Metal-organic frameworks (MOFs) are crystalline porous structures constructed by joining metal-containing units [secondary building units (SBUs)] with organic linkers by strong bonds.[1] In the past twenty five years, MOFs have attracted great attention with exponential growth of research, owing to their tunable chemical environment for applications in areas such as gas separation and catalysis.[2–4] These applications are dependent on the choice of building blocks and synthetic procedures, size and shape of pores in MOFs and the interactions between guests and frameworks. In particular, the stereochemistry of the framework plays a vital role in determining properties of MOFs and has wide applications in asymmetric catalysis, enantioselective separation, and structure determinations of small molecules with absolute configurations.[5–17] Thus, the study of MOFs with absolute structures is important in the field of MOF chemistry.

Absolute structures are divided into two categories: chiral structures, and achiral but non-centrosymmetric structures.[18] While the MOFs of the second kind haven't been systematically studied, chiral MOFs are of broad interest and many attempts toward the syntheses of chiral MOFs have been reported. The synthetic strategies of obtaining such MOFs include: (i) direct synthesis of MOFs by using chiral ligands,[19–22] (ii) post-synthetic modification of achiral MOFs with chiral auxiliaries,[23–26] (iii) chiral induction of MOFs with achiral building units by using chiral templates.[27–29] These synthetic methods have been extensively developed, however, most require the use of chiral species. Compared with using chiral ligands or templates, it is more challenging to synthesize chiral MOFs from achiral starting materials since the chirality of MOFs is relatively unpredictable during the synthesis. As there are limited reports in this research topic,[30–32] this is also an important topic as enantiopure compounds are not always easy to obtain.

Here, we report the synthesis and structure of a new Al-based MOF with absolute structure, MOF-829 [$Al_3(\mu_3\text{-}O)(OH)(H_2O)_2(BTB)_2$, BTB = 1,3,5-benzenetribenzoate]. By comparing it with a reported chiral MOF, MOF-520 [$Al_8(\mu\text{-}OH)_8(HCOO)_4(BTB)_4$], we analyze the role of building units (SBUs and linkers) and topology in producing MOFs with absolute structures, and further the influence of synthetic

---

[a] *H. Wang,+ X. Pei,+ O. M. Yaghi*
Department of Chemistry, University of California-Berkeley,
Berkeley, California, 94720, U.S.A.
E-mail: yaghi@berkeley.edu

[b] *H. Wang,+ X. Pei,+ O. M. Yaghi*
Kavli Energy NanoSciences Institute
Berkeley, California, 94720, U.S.A.

[c] *D. M. Proserpio*
Dipartimento di Chimica, Università degli Studi di Milano
Milano, 20133, Italy

[d] *D. M. Proserpio*
Samara Center for Theoretical Materials Science (SCTMS),
Samara State Technical University,
Samara, 443100, Russia

[+] *Co-first authors, with equal contribution.*

Supporting information for this article is available on the WWW under https://doi.org/10.1002/ijch.202100102

procedures on obtaining such MOFs without the need of auxiliary chiral inducers. These two MOFs are synthesized from the same metal ions and organic linkers, however, careful tuning of the modulators in the synthesis leads to the formation of different SBUs with and without intrinsic chirality, and thus directing the formation of MOFs with distinct structures.

2. Experimental Section

2.1 Materials and Methods

Aluminum chloride ($AlCl_3$) and formic acid were obtained from Acros Organics. 1,3,5-benzenetribenzoic acid (H_3BTB) and *N*,*N*-diethylformamide (DEF) were purchased from TCI America. All chemicals were used without further purification.

The topology of MOF-829 was analyzed by the following procedure: (1) for checking the topology in RCSR database,[33] the single-crystal structure of MOF-829 was first reduced by substituting SBUs and linkers with atoms at their centers-of-gravity. The connectivity was then calculated in ToposPro[34] based on close contact. The obtained adjacent matrix was further rectified to make sure it matches the chemical connectivity in the original MOF structure. The established reduced structure was exported into .cgd file and then imported into Systre[35] for topology analysis. (2) To check the underlying net of MOF-829 in the TTD database,[36] the CIF file was analyzed by ToposPro[34] and TopCryst.[37]

2.2 Synthetic Procedure

Preparation of MOF-829: $AlCl_3$ (3.3 mg, 0.0251 mmol) and H_3BTB (7.4 mg, 0.0168 mmol) were dissolved in a solvent mixture of DEF/formic acid (1.788 mL/0.112 mL) in a 4 mL pressure tube. The mixture was heated at 160 °C for one day and block colorless crystals were obtained.

2.3 Determination and Refinement of the Single-Crystal X-Ray Structure

The single-crystal X-ray structure of MOF-829 was measured on a Rigaku XtaLAB P200 equipped with a MicroMax 007HF rotating anode and a Pilatus 200 K hybrid pixel array detector. A single crystal of MOF-829 of 0.22 × 0.16 × 0.15 mm was mounted on a capillary base and placed in a 150 K nitrogen cold stream (slightly above the melting point of DEF) from Oxford Cryosystem 700, then measured by Cu Kα radiation with omega scans. The data was integrated using CrysAlis Pro software package and scaled by the SCALE3 ABSPACK.[38] The space group was determined to be $Pca2_1$. The primary structure solution was obtained using SHELXT-2018/02[39] and the full-matrix least-square refinement on F^2 was done by SHELXL-2018/03,[40] both using the Olex2[41] software package. All the non-hydrogen atoms were refined anisotropically and hydrogens were placed at geometrically-calculated positions. The structure was refined as an inversion twin (detailed discussion in section 3.3). Olex2 solvent mask procedure[42] was applied; the masked volume and total number of masked electrons are 22408.0 Å^3 and 6666.9 e^-, respectively. The percentage of void space is 76.8%. Weighing scheme was refined to converge at the end. Detailed statistics on the data quality and the quality of structure solution are summarized in Table 1. The crystallographic information file (CIF) of the structure can be accessed from Cambridge Structure Database (CSD) via deposition number 2101022.

Table 1. Measurement details, data quality and refinement quality of the single-crystal structure of MOF-829.

	Before SQUEEZE	After SQUEEZE
Formula	$Al_6C_{108}O_{32}H_{70}\cdot x(DMF)$	$Al_6C_{108}O_{32}H_{70}$
Formula weight	2041.52 + x(DMF)	2041.52
Temperature/K	150	150
Crystal system	orthorhombic	orthorhombic
Space group	$Pca2_1$	$Pca2_1$
a/Å	34.5751(3)	34.5751(3)
b/Å	18.3942(2)	18.3942(2)
c/Å	45.8595(4)	45.8595(4)
Volume/Å^3	29165.8(5)	29165.8(5)
Z	4	4
ρ_{calc} (g/cm^3)	0.465	0.465
μ/mm^{-1}	0.450	0.450
F(000)	4208.0	4208.0
Crystal size/mm^3	0.22 × 0.16 × 0.15	0.22 × 0.16 × 0.15
Radiation	Cu Kα (λ = 1.54178 Å)	Cu Kα (λ = 1.54178 Å)
2θ range for data collection/°	5.774 to 139.052	5.774 to 139.052
Index ranges	$-41 \le h \le 42$ $-22 \le k \le 22$ $-54 \le l \le 55$	$-41 \le h \le 42$ $-22 \le k \le 22$ $-54 \le l \le 55$
Reflections collected	795662	795662
Independent reflections	54113 (R_{int} = 0.0685, R_{sigma} = 0.0274)	54113 (R_{int} = 0.0685, R_{sigma} = 0.0274)
Restrains and parameters	1/1316	1/1316
Goodness-of-fit on F^2	1.670	0.960
Final R indexes [I > = 2σ (I)]	R_1 = 0.1629 wR_2 = 0.3663	R_1 = 0.0295 wR_2 = 0.0761
Final R indexes [all data]	R_1 = 0.1780 wR_2 = 0.3753	R_1 = 0.0364 wR_2 = 0.0792
Largest diff. peak/hole/e Å^{-3}	1.79/−0.74	0.38/−0.31
Flack parameter	0.40(5)[a]	0.434(11)
Hooft parameter		0.425(2)
Parsons parameter		0.441(4)

[a] The parameters before SQUEEZE intrisically contains errors caused by solvent scattering. The values and their standard uncertainties should be viewed critically.

3. Results and Discussions

3.1 Synthesis and Structure of MOF-829 and MOF-520

MOF-829 is built from a trinuclear SBU [$Al_3(\mu_3$-$O)(OH)(H_2O)_2(–COO)_6$]: One of the six corners in each AlO_6 octahedron is shared with the other two octahedra through a μ_3-oxygen atom, four of corners are bridged by carboxylate groups with adjacent aluminum ions, and the last corner is capped by either OH^- or H_2O (the number of hydrogen is derived based on charge balance). Each SBU is connected to six carboxylate groups from six linkers, forming the extended structure in the newly identified 3,6-connected net (Figure 1 and 4b).

MOF-520 was obtained from the same metal ions [Al(III)] and linkers (BTB) as MOF-829 however different synthetic conditions.[10] The metal source used in this synthesis is $Al(NO_3)_3 \cdot 9H_2O$, with more water of hydration compared to the anhydrous $AlCl_3$ used for MOF-829. Finely-tuned trace amount of water was also added to match the required water content for producing MOF-520. With a lower reaction temperature (140 °C) and the presence of higher water content in the synthetic media, the Al^{3+} ions likely went through a milder hydrolysis process and longer aggregation time.[43,44] As

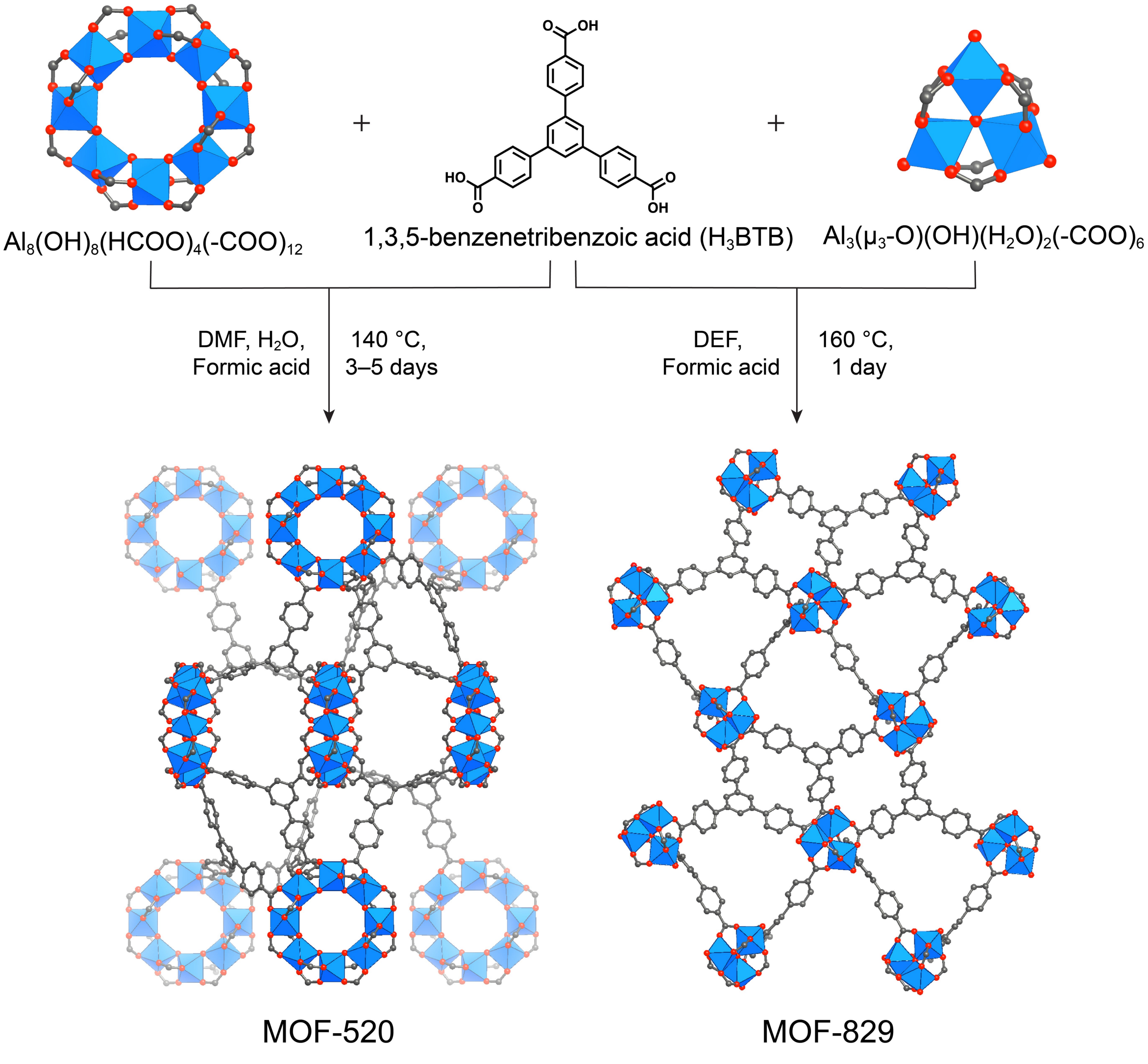

Figure 1. Synthesis and structures of MOF-520 and MOF-829 (CSD deposition number: 1488944, 1488951 and 2101022. The two structures of MOF-520 are with different chiralities, which will be discussed in detail in Section 3.2). MOF-520 is built from SBU [$Al_8(OH)_8(HCOO)_4(–COO)_{12}$] and BTB linker. Each SBU is linked by twelve BTB linkers, and each BTB linker is bound to three different SBUs. The structure of MOF-520 is formed in 3,12-connected **fon** topology. MOF-829 is comprised of the SBU, [$Al_3(\mu_3$-$O)(OH)(H_2O)_2(–COO)_6$], and BTB linker. Each SBU is connected to six carboxylate groups from six BTB linkers, forming the extended structure in 3,6-connected 3,3,3,3,6,6T23 net. Color code: Al, blue; O, red; C, gray. H atoms are omitted for clarity.

a result, the SBUs of MOF-520 are larger and composed of eight circularly-arranged aluminum octahedra. Every two adjacent aluminum atoms share corners through μ-OH groups, and in addition are bridged by two carboxylate groups. The total of sixteen bridging carboxylate groups of each SBU come from both formate and BTB linkers. Each SBU is linked by twelve BTB linkers, and each BTB linker binds to three different SBUs. The structure of MOF-520 is therefore formed in the 3,12-connected **fon** topology (Figure 1 and 4a).[45]

3.2 Absolute Structure of MOF-520

As a MOF that crystallizes in enantiopure single crystals, the absolute configurations of MOF-520 have already been reported in our previous study[8,10] and demonstrated great application in facilitating the single-crystal structure determination of complex chiral compounds. The notation of the enantiomorphs of MOF-520 in the previous work was simply based on the conformations of the BTB linkers (Λ and Δ; Figure 2a, b) as the achiral H$_3$BTB molecules adopt chiral atomic arrangements in MOF-520 crystals, however, the chirality of SBUs was not discussed. The origin of the absolute configuration of the SBUs in MOF-520 can be understood from two aspects. The first is the arrangement of the coordinating formate groups: it follows the chiral site symmetry of the SBU, 222 (D_2) without having additional local symmetry operations.[46] On the second aspect, the chiral arrangement of formate groups and other carboxylate from linkers decides the coordination asymmetry of the aluminum octahedra, thus allowing the notation of the absolute configuration of the SBUs through the nomenclature for octahedral chiral complexes (Figure 2c, left). A traditional approach for analyzing the stereochemistry of coordination centers was performed based on IUPAC recommendation.[47] As a result, there are three kinds of aluminum octahedra in the crystal structure: the coordination spheres of Al1 and Al3 contain mirror planes (not considering the absolute geometry of the ligands) thus no absolute configuration, while the sequence of ligand arrangement [assigned by Cahn-Ingold-Prelog (CIP) convention] determines the chirality to Al2 octahedron (Figure 2c, middle and right). It is found that only *A* configuration of Al2 exists in Λ-MOF-520, meanwhile only *C* configuration of Al2 exists in Δ-MOF-520. Therefore, the chirality of a MOF-520 crystal is not only determined by the conformation of the linker, but also the absolute configuration of the SBU.

3.3 Absolute Structure of MOF-829

Unlike the SBU of MOF-520, the tri-aluminum SBU is traditionally viewed as an centrosymmetric unit with point symmetry of $\bar{6}2m$ (D_{3h}). Although there is a slight deviation on the geometry of the SBUs in MOF-829 that the aluminum octahedra all rotates clockwise/anticlockwise for 5–7 degrees around the μ_3-O-Al axes (Figure 3a), they are still close to their ideal geometry and the SBU is thus considered as pseudo-centrosymmetric. The BTB linker in the crystal

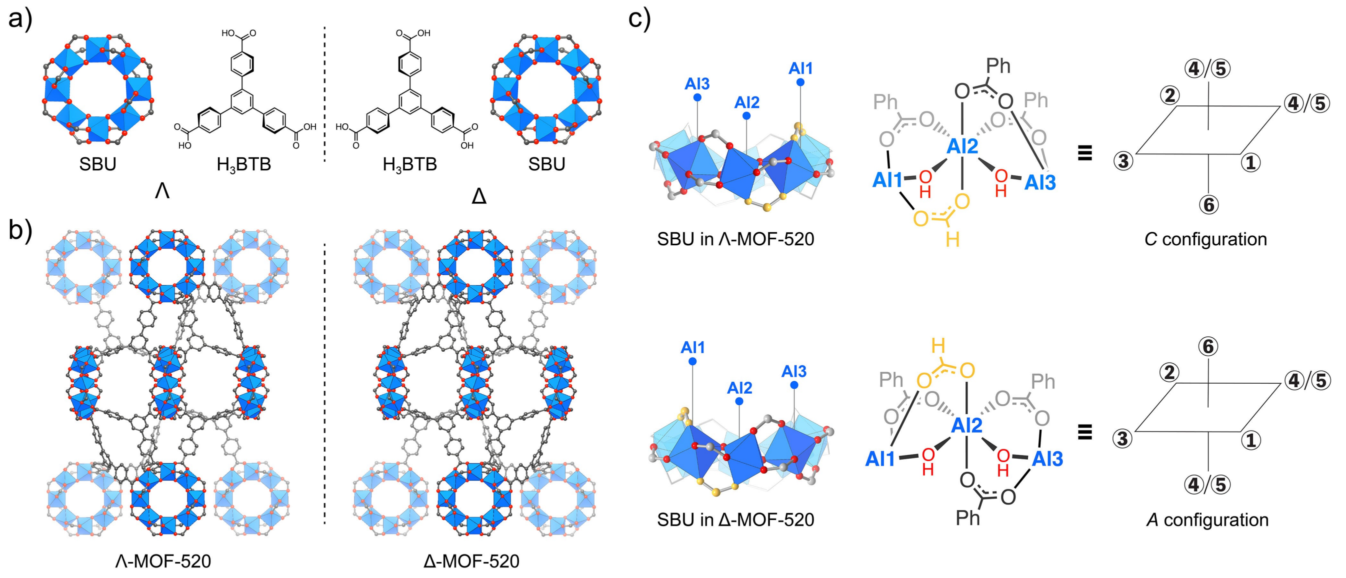

Figure 2. a) Illustration of the SBUs and BTB linkers in Λ- and Δ-MOF-520. b) The structure of Λ- and Δ-MOF-520. Color code: Al, blue; O, red; C, gray. H atoms are omitted for clarity. Dashed lines in (a) and (b) indicates configurations are mirrored to each other. c) Left: Al ions of different chemical environments and their locations in SBU. Middle: the coordination octahedra of Al2 in both MOFs, formate groups are highlighted in yellow and the linkers on the back are colored in gray. Right: the ligand priority of the two kinds of Al2 octahedron determined by the CIP rule are numbered in corresponding schemes. Structures of Δ- and Λ-MOF-520 can be accessed from CSD via deposition number 1488944 and 1488951, respectively.

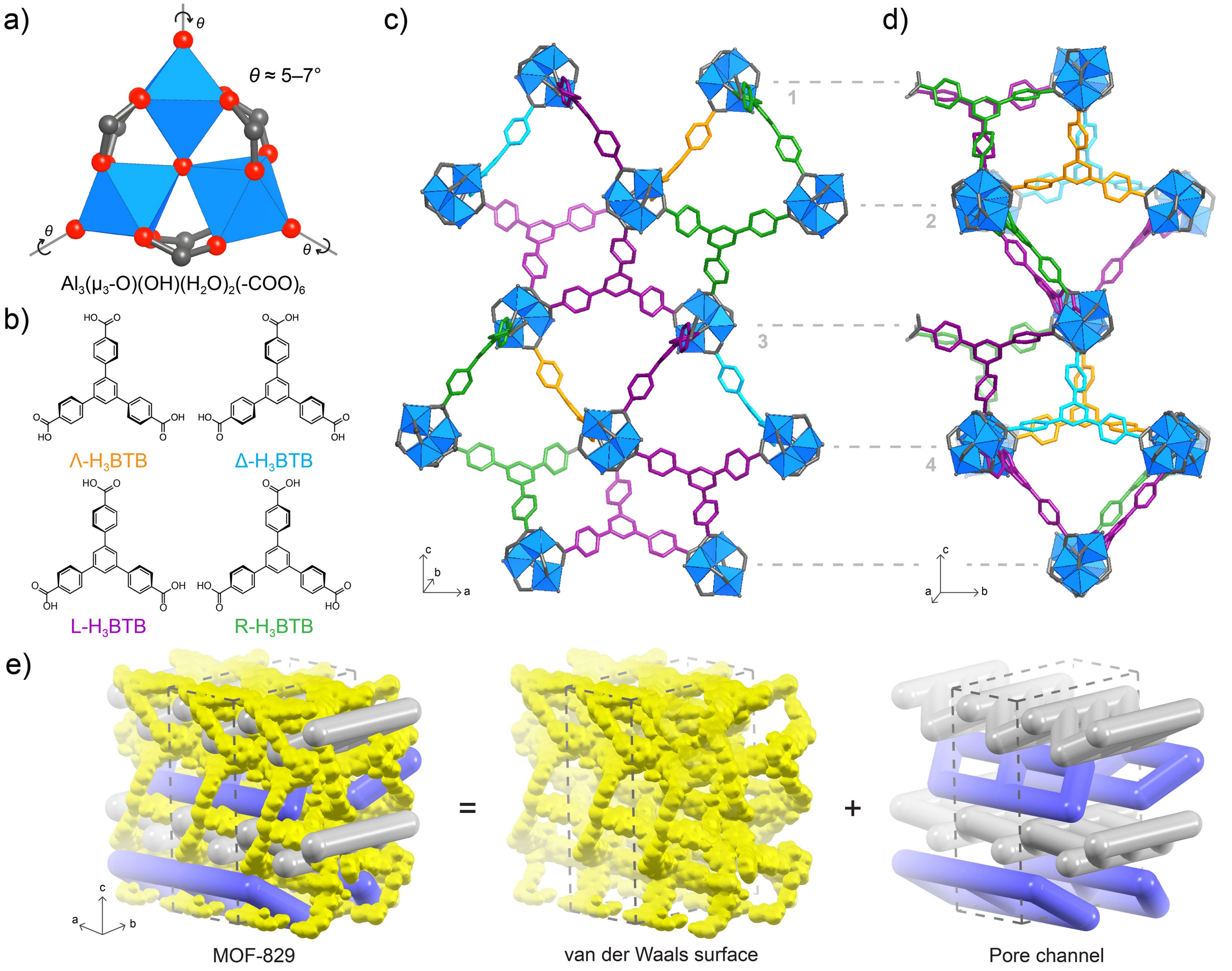

Figure 3. a) The tri-aluminum SBU in MOF-829. b) The BTB linker adopts four kind of conformations (Λ, Δ, L, and R) in MOF-829. c) The arrangement of Λ-, Δ-, L-, and R-H$_3$BTB linkers in MOF-829 viewed along the *b* axis. The linkers are arranged in four layers separated by Al SBUs, where the first and the third layers consist of all four conformations of the linkers, while the second and the fourth layers only comprise L- and R-BTB linkers. (d) The arrangement of Λ-, Δ-, L-, and R-BTB linkers in MOF-829 viewed along the *a* axis. Color code: Al, blue; O, red in (a), gray in (c) and (d); C, gray. Λ-BTB linker, light orange; Δ-BTB linker, sky blue; L-BTB linker, violet; R-BTB linker, green. H atoms are omitted for clarity. e) Illustration of the pore channel structures of MOF-829. Grey cylinders represent the interconnected pore channels in layer 1 and layer 3, while violet cylinders represent the interconnected pore channels in layer 2 and 4. The diameter of the cylinders is *ca.* 7.5 Å. The grey and violet channels further connect at where the cylinder surfaces intersect, forming a 3D channel framework. Dashed lines outline the unit cell. The CSD deposition number of MOF-829 is 2101022.

structure of MOF-829 appears in four kinds of conformations (Figure 3b). While two of them are of the same propeller-shape as in MOF-520 (Λ and Δ), there are two additional chiral conformations that can be regarded as one of the propeller blades flipping to the opposite orientation (annotated as L and R in the following text). Despite having two pairs of enantiomers, all of the four conformations of BTB present in the same crystal of MOF-829 due to the existence of glide planes in the space group. The combination of racemic linkers conformations and pseudo-centrosymmetric SBUs derives the achiral structure of MOF-829. However, the non-centrosymmetric space group (*Pca*2_1) indicates that it still has an absolute structure, although there are no enantiomorphs.[48]

Determination of the absolute structure was carefully performed. The diffraction data collections at shorter X-ray wavelengths indicated that such energies cannot generate sufficient anomalous scattering to differentiate the intensities of Friedel pairs (FRIEDIF = 38 at $\lambda = 0.7288$ Å, calcualted by PLATON),[49,50] therefore, longer wavelengths (Cu Kα) were chosen to obtained the reported dataset (FRIEDIF = 166).[51] Additionally, the data collection strategy covered full sphere of reciprocal space so that it ensured a Friedel coverage of

98 % for a Flack parameter with reliable standard uncertainty.[18a] The correct determination of the Flack parameter is also confirmed by its agreement with the Hooft and the Parsons parameters (Table 1).[52] The relatively small standard uncertainty obtained with good measurement rules out the possibility of that the absolute structure is ambigious,[18a,53] furthermore the obtained structure was carefully inspected and no additional symmetry (especially inversion symmetry) was found. Thus, the structure is not a centrosymmetric structure wrongly solved in non-centrosymmetric space group, and the relatively large Flack parameter is a result of inversion twinning. In fact, the non-centrosymmetric structural feature can be thoroughly understood from the arrangement of the building units along the *c* axis, the polar axis of $Pca2_1$. A structure fragment in one unit cell range representing these features is illustrated in Figure 3c and 3d. When viewing from the *b* axis, the linkers are arranged in four layers separated by Al SBUs, where the first and the third layers consist of all four conformations of the linkers, while the second and the fourth layers only comprise L- and R-BTBs (Figure 3c). The L-/R-BTB linkers are aligned in "V" shapes when viewing along *a* axis, and inverted V shapes aren't present in the structure (Figure 3d). Similarly, the Λ-/Δ-BTB linkers are uniformly directly along the *c* axis, while all the L-/R-BTB linkers align to the opposite direction. The different alignment of the BTB linkers further creates two sets of 2D pore channel networks, arranging in a non-centrosymmetic fashion (Figure 3e, illustrated by grey and violet cylinders). The 2D networks futher interconnect to form the 3D pore channel framework of MOF-829. As a conclusion, the collective arrangement of the linkers with absolute conformations determines the absolute structure of MOF-829, unlike in MOF-520 that it is the presence of one in the pair of enantiomers that determines the absolute configuration of the MOF.

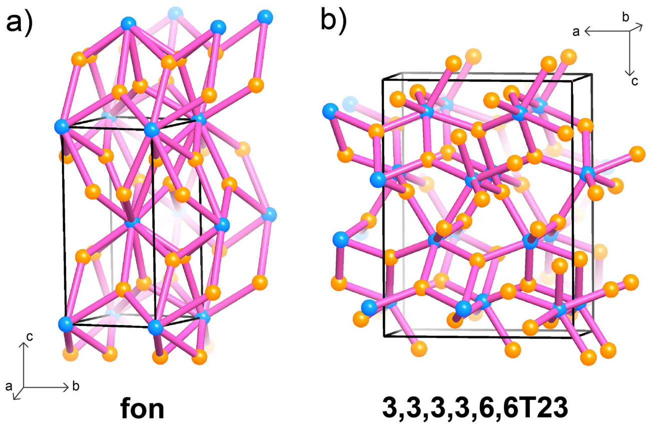

Figure 4. a) Illustration of the **fon** topology in its maximum embedding symmetry ($P4_2/nmc$). The 3-connected and 12-connected nodes are colored in yellow and blue, respectively. b) Illustration of the 3,3,3,3,6,6T23 net in its maximum embedding symmetry ($Pca2_1$). The 3-connected and 6-connected nodes are colored in yellow and blue, respectively. All kinds of edges in both topologies are uniformly colored in magenta.

3.4 The Relationship between the Topologies and the Absolute Structures

The arrangement of linkers and SBUs inside a MOF can be well-described by the concept of topology in reticular chemistry. Therefore, we further investigate the topology of both MOFs searching for a possible relation with the formation of MOFs with absolute structures. Although the topology of MOF-829 was not included in the RCSR database, we analyzed the structure following IUPAC guidelines[54] with Systre and ToposPro: the cluster representation gives a known underlying net with point symbol $(4\cdot6^2)(4\cdot6^9\cdot8^5)(6^3)$ named 3,3,3,3,6,6T23 (Figure 4b). The Samara Topological Data Center[36,37] shows four isoreticular compounds with refcodes TOVJAR,[55] OYEWEW,[56] MUKDUU,[57] LURJUG.[58] The net is composed of six kinds of nodes (two 6-connected and four 3-connected) and twelve kinds of edges. The maximum symmetry embedding of the 3,3,3,3,6,6T23 net is determined to be $Pca2_1$, the same as for MOF-829. As the structures possessing one topology can only lie in a space group that is the subgroup of the highest possible symmetry, any MOF with this topology must be in a non-centrosymmetric space group as there is no inversion center in the space group $Pca2_1$ and any of the subgroups. Although there are many cases of centrosymmetric molecules crystallizing in non-centrosymmetric space groups,[59,60] it cannot happen to MOFs as the inversion center will become global symmetry once it appears in a periodically extended structure. Therefore, we conclude that it is the net topology of MOF-829 that determines the formation of this MOF with an absolute structure.

In comparison, the **fon** topology of MOF-520 has the maximum embedding symmetry of $P4_2/nmc$, a centrosymmetric space group (Figure 4a).[33,61] The constructing units therefore have to be carefully chosen if a chiral structure is desired. H_3BTB is likely insufficient to act as the only strong structure-directing linker as it can possess many flexible conformations, but the presence of a chiral SBU at the same time increase the chance of forming a chiral structure. Indeed, there is still possibility that a meso compound can be formed even though building units with absolute configurations are chosen. In this case, the dimensions of the building units and the angles between them when forming a structure are also critical for the formation of an enantiopure structure.

4. Conclusion and Outlook

From this comparative study between MOF-829 and MOF-520, we conclude that the underlying topology can determine the formation of a MOF with absolute structure if the topology itself is already non-centrosymmetric or chiral. If the topology itself is centrosymmetric, building units with potential absolute configurations have to be chosen. The choice of organic linkers with potential absolute conformations is rather straightforward, but the choice of SBUs with absolute structures from careful tuning of synthetic conditions hasn't been pursued. However, there are still rich SBU chemistry to be explored, especially for ions that can undergo complicated controlled hydrolysis such as Al and Ti. A large number of ion-oxo clusters of these elements have been reported that can be potential SBUs of MOFs,[43,62–66] meanwhile, there are also SBUs such as the octa-aluminum SBU in MOF-520 that never had such chiral configurations reported in individual clusters. Therefore, we envision that there is significant potential in pure synthetic-driven formation of SBUs with absolute configurations yet with no chiral auxiliary.

Acknowledgements

We acknowledge the NIH (Grant S10-RR027172) for financial support of the X-ray crystallographic facility at UC Berkeley, and Dr. Nicholas Settineri for the support on using the facility. H. W. and X. P. thank Hao Lyu for the helpful discussions and suggestions on the manuscript. X. P. thanks Dr. E. A. Kapustin for discussions on the chirality of MOF-520.

References

[1] O. M. Yaghi, M. J. Kalmutzki, C. S. Diercks, *Introduction to Reticular Chemistry: Metal-Organic Frameworks and Covalent Organic Frameworks*, Wiley-VCH, Weinheim **2019**.

[2] H. Furukawa, K. E. Cordova, M. O'Keeffe, O. M. Yaghi, *Science* **2013**, *341*, 1230444.

[3] J. Lee, O. K. Farha, J. Roberts, K. A. Scheidt, S. T. Nguyen, J. T. Hupp, *Chem. Soc. Rev.* **2009**, *38*, 1450–1459.

[4] H. Wang, Z. Shi, J. Yang, T. Sun, B. Rungtaweevoranit, H. Lyu, Y.-B. Zhang, O. M. Yaghi, *Angew. Chem. Int. Ed.* **2021**, *133*, 3459–3463.

[5] A. L. Nuzhdin, D. N. Dybtsev, K. P. Bryliakov, E. P. Talsi, V. P. Fedin, *J. Am. Chem. Soc.* **2007**, *129*, 12958–12959.

[6] L. Ma, C. Abney, W. Lin, *Chem. Soc. Rev.* **2009**, *38*, 1248–1256.

[7] Y. Liu, W. Xuan, Y. Cui, *Adv. Mater.* **2010**, *22*, 4112–4135.

[8] S. Lee, E. Kapustin, O. M. Yaghi, *Science* **2016**, *353*, 808–811.

[9] Y. Inokuma, S. Yoshioka, J. Ariyoshi, T. Arai, Y. Hitora, K. Takada, S. Matsunaga, K. Rissanen, M. Fujita, *Nature* **2013**, *495*, 461–466.

[10] X. Pei, H.-B. Bürgi, E. A. Kapustin, Y. Liu, O. M. Yaghi, *J. Am. Chem. Soc.* **2019**, *141*, 18862–18869.

[11] R. Vaidhyanathan, S. S. Iremonger, G. K. H. Shimizu, P. G. Boyd, S. Alavi, T. K. Woo, *Science* **2010**, *330*, 650–653.

[12] A. Cadiau, K. Adil, P. Bhatt, Y. Belmabkhout, M. Eddaoudi, *Science* **2016**, *353*, 137–140.

[13] L. Li, R. Lin, R. Krishna, H. Li, S. Xiang, H. Wu, J. Li, W. Zhou, B. Chen, *Science* **2018**, *362*, 443–446.

[14] M. H. Mohamed, Y. Yang, L. Li, S. Zhang, J. P. Ruffley, A. Jarvi, S. Saxena, G. Veser, J. Johnson, N. L. Rosi, *J. Am. Chem. Soc.* **2019**, *141*, 13003–13007.

[15] J. Lee, O. K. Farha, J. Roberts, K. A. Scheidt, S. T. Nguyen, J. T. Hupp, *Chem. Soc. Rev.* **2009**, *38*, 1450–1459.

[16] K. Manna, T. Zhang, W. Lin, *J. Am. Chem. Soc.* **2014**, *136*, 6566–6569.

[17] Y.-S. Wei, M. Zhang, R. Zou, Q. Xu, *Chem. Rev.* **2020**, *120*, 12089–12174.

[18] a) H. D. Flack, *Helv. Chim. Acta* **2003**, *86*, 905–921; b) H. D. Flack, G. Barnerdinelli, *Chirality* **2008**, *20*, 681–690.

[19] J. S. Seo, D. Whang, H. Lee, S. Jun, J. Oh, Y. Jeon, K. Kim, *Nature* **2000**, *404*, 982–986.

[20] L. Ma, J. M. Falkowski, C. Abney, W. Lin, *Nat. Chem.* **2010**, *2*, 838–846.

[21] M. M. Wanderley, C. Wang, C. Wu, W. Lin, *J. Am. Chem. Soc.* **2012**, *134*, 9050–9053.

[22] Z. Gu, C. Zhan, J. Zhang, X. H. Bu, *Chem. Soc. Rev.* **2016**, *45*, 3122–3144.

[23] M. Banerjee, S. Das, M. Yoon, H. J. Choi, M. H. Hyun, S. M. Park, G. Seo, K. Kim, *J. Am. Chem. Soc.* **2009**, *131*, 7524–7525.

[24] S. J. Garibay, Z. Wang, K. K. Tanabe, S. M. Cohen, *Inorg. Chem.* **2009**, *48*, 7341–7349.

[25] S. C. Jones, C. A. Bauer, *J. Am. Chem. Soc.* **2009**, *131*, 12516–12517.

[26] R. J. Marshall, S. L. Griffin, C. Wilson, R. S. Forgan, *Chem. Eur. J.* **2016**, *22*, 4870–4877.

[27] C. J. Kepert, T. J. Prior, M. J. Rosseinsky, *J. Am. Chem. Soc.* **2000**, *122*, 5158–5168.

[28] Z. Lin, A. M. Z. Slawin, R. E. Morris, *J. Am. Chem. Soc.* **2007**, *129*, 4880–4881.

[29] S. Y. Zhang, D. Li, D. Guo, H. Zhang, W. Shi, P. Cheng, L. Wojtas, M. J. Zaworotko, *J. Am. Chem. Soc.* **2015**, *137*, 15406–15409.

[30] M. C. di Gregorio, L. J. W. Shimon, V. Brumfeld, L. Houben, M. Lahav, M. E. van der Boom, *Nat. Commun.* **2020**, *11*, 380.

[31] a) T. M. McDonald, W. R. Lee, J. A. Mason, B. M. Wiers, C. S. Hong, J. R. Long, *J. Am. Chem. Soc.* **2012**, *134*, 7056–7065; b) J. D. Martell, L. B. Porter-Zasada, A. C. Forse, R. L. Siegelman, M. I. Gonzalez, J. Oktawiec, T. Runčevski, J. Xu, M. Srebro-Hooper, P. J. Milner, K. A. Colwell, J. Autschbach, J. A. Reimer, J. R. Long, *J. Am. Chem. Soc.* **2017**, *139*, 16000–16012.

[32] C. Castillo-Blas, V. A. de la Peña-O'Shea, I. Puente-Orench, J. R. de Paz, R. Sáez-Puche, E. Gutiérrez-Puebla, F. Gándara, Á. Monge, *Sci. Adv.* **2017**, *3*, e1700773.

[33] M. O'Keeffe, M. A. Peskov, S. J. Ramsden, O. M. Yaghi, *Acc. Chem. Res.* **2008**, *41*, 1782–1789.

[34] V. A. Blatov, A. P. Shevchenko, D. A. Proserpio, *Cryst. Growth Des.* **2014**, *14*, 3576–3586.

[35] O. Delgado-Friedrichs, M. O'Keeffe *Acta Crystallogr. Sect. A* **2003**, *59*, 351–360.

[36] E. V. Alexandrov, A. P. Shevchenko, V. A. Blatov, *Cryst. Growth Des.* **2019**, *19*, 2604–2614.

[37] *TopCryst - The Samara Topological Data Center* (**2020**) [online]. Available from: https://topcryst.com [accessed Aug 5, 2021].

[38] CrysAlis Pro 1.171.40.53, Rigaku Oxford Diffraction, **2019**.

[39] G. M. Sheldrick, *Acta Crystallogr. Sect. A* **2015**, *71*, 3–8.

[40] G. M. Sheldrick, *Acta Crystallogr. Sect. C* **2015**, *71*, 3–8.

[41] O. V. Dolomanov, L. J. Bourhis, R. J. Gildea, J. A. K. Howard, H. Puschmann, *J. Appl. Crystallogr.* **2009**, *42*, 339–341.

[42] P. van der Sluis, A. L. Spek, *Acta Crystallogr. Sect. A* **1990**, *46*, 194–201.

[43] W. H. Fang, L. Zhang, J. Zhang, *Chem. Soc. Rev.* **2018**, *47*, 404–421.

[44] L. Geng, C.-H. Liu, S.-T. Wang, W.-H. Fang, J. Zhang, *Angew. Chem. Int. Ed.* **2020**, *59*, 16735–16740; *Angew. Chem.* **2020**, *132*, 16878–16883.

[45] E. A. Kapustin, S. Lee, A. S. Alshammari, O. M. Yaghi, *ACS Cent. Sci.* **2017**, *3*, 662–667.

[46] *International Tables for Crystallography Vol. A* (Eds.: M. I. Aroyo), Wiley-VCH, Weinheim **2016**, pp. 410–411.

[47] *Nomenclature of Inorganic Chemistry - IUPAC Recommendations* (Eds.: N. G. Connelly, T. Damhus, R. M. Hartshorn, A. T. Hutton), Royal Society of Chemistry, Cambridge **2005**, pp. 189–190.

[48] *Online Dictionary of Crystallography, Absolute structure* (**2017**) [online]. Available from: https://dictionary.iucr.org/Absolute_structure [Accessed June 29, 2021].

[49] A. L. Spek, *J. Appl. Crystallogr.* **2003**, *36*, 7–13.

[50] H. D. Flack, G. Barnerdinelli, *Acta Crystallogr. Sect. A* **2008**, *64*, 484–493.

[51] S. Parsons, *Tetrahedron: Asymmetry* **2017**, *28*, 1304–1313.

[52] D. J. Watkin, R. I. Cooper, *Acta Crystallogr. Sect. B* **2016**, *72*, 661–683.

[53] D. J. Watkin, R. I. Cooper, *Chemistry (Basel, Switz.)* **2020**, *2*, 796–804.

[54] C. Bonneau, M. O'Keeffe, D. M. Proserpio, V. A. Blatov, S. R. Batten, S. A. Bourne, M. S. Lah, J.-G. Eon, S. T. Hyde, S. B. Wiggin, L. Öhrström, *Cryst. Growth Des.* **2018**, *18*, 3411–3418.

[55] D. Feng, K. Wang, Z. Wei, Y.-P. Chen, C. M. Simon, R. Arvapally, R. L. Martin, M. Bosch, T.-F. Liu, S. Fordham, D. Yuan, M. A. Omary, M. Haranczyk, B. Smit, H.-C. Zhou, *Nat. Commun.* **2014**, *5:5723*, doi: 10.1038/ncomms6723.

[56] a) J. Tian, *CSD Communication*, **2016**; b) C.-S. Liu, C.-X. Sun, J.-Y. Tian, Z.-W. Wang, H.-F. Ji, Y.-P. Song, S. Zhang, Z.-H. Zhang, L.-H. He, M. Du, *Biosens. Bioelectron.* **2017**, *91*, 804–810.

[57] L.-Z. Dong, L. Zhang, J. Liu, Q. Huang, M. Lu, W.-X. Ji, Y.-Q. Lan, *Angew. Chem. Int. Ed.* **2020**, *59*, 2659–2663; *Angew. Chem.* **2020**, *132*, 2681–2685.

[58] H.-J. Lv, Y.-P. Li, Y.-Y. Xue, Y.-C. Jiang, S.-N. Li, M.-C. Hu, Q.-G. Zhai, *Inorg. Chem.* **2020**, *59*, 4825–4834.

[59] F. H. Herbstein, F. R. L. Schoening, *Acta Crystallogr.* **1957**, *10*, 657–663.

[60] E. Pidcock, *Chem. Commun.* **2005**, 3457–3459.

[61] O. Delgado-Friedrichs, M. O'Keeffe, *RCSR database: fon topology.* Available from: http://rcsr.net/nets/fon [Accessed June 31, 2021].

[62] R. Murugavel, S. Kuppuswamy, *Angew. Chem. Int. Ed.* **2006**, *45*, 7022–7026; *Angew. Chem.* **2006**, *118*, 7180–7184.

[63] C. Rong, Z. Yu, Q. Wang, S.-T. Zheng, C.-Y. Pan, F. Deng, G.-Y. Yang, *Inorg. Chem.* **2009**, *48*, 3650–3659.

[64] K. S. Lokare, N. Frank, B. Braun-Cula, I. Goikoetxea, J. Sauer, C. Limberg, *Angew. Chem. Int. Ed.* **2016**, *55*, 12325–12329; *Angew. Chem.* **2016**, *128*, 12513–12517.

[65] W. Xuan, C. Ye, M. Zhang, Z. Chen, Y. Cui, *Chem. Sci.* **2013**, *4*, 3154–3159.

[66] Y. Sun, D.-F. Lu, Y. Sun, M.-Y. Gao, N. Zheng, C. Gu, F. Wang, J. Zhang, *ACS Materials Lett.* **2021**, *3*, 64–68.

Manuscript received: September 9, 2021
Revised manuscript received: October 4, 2021
Version of record online: ■■, ■■

RESEARCH ARTICLE

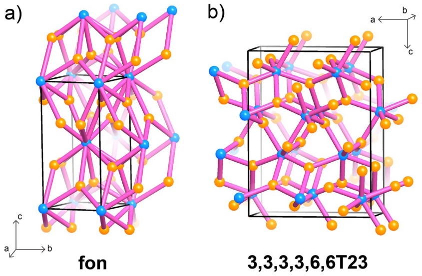

fon

3,3,3,3,6,6T23

*H. Wang, X. Pei, D. M. Proserpio, O. M. Yaghi**

1 – 9

Design of MOFs with Absolute Structures: A Case Study